Polymer Chemistry

ROYAL SOCIETY OF CHEMISTRY

PAPER

View Article Online
View Journal | View Issue

Cite this: *Polym. Chem.*, 2023, **14**, 2838

Polymers from sugars and isothiocyanates: ring-opening copolymerization of a D-xylose anhydrosugar oxetane†

Ella F. Clark, [a,c] Gabriele Kociok-Köhn, [b] Matthew G. Davidson[a,c] and Antoine Buchard *[a,c]

A D-xylose 3,5-anyhydrosugar (**D-Ox**) has been applied in the ring-opening copolymerisation (ROCOP) with isothiocyanates to form alternating AB-type copolymers with imidothiocarbonate linkages ($M_n \geq$ 34 900 g mol^{-1}). Catalysed by an Al(III)-based aminotrisphenolate complex, ROCOP proceeds with high selectivity with four aromatic isothiocyanates, including di-isothiocyanates used for crosslinking, to form thermally robust polymers ($T_{d,5\%}$ >228 °C) with a range of high glass-transition temperatures (76–134 °C). Kinetic studies show a reaction order of two with respect to the binary catalytic system, and a first order with respect to **D-Ox**. When using an Al(III) porphyrin complex as catalyst, the reactivity can be tailored to form exclusively a non-polymerisable cyclic thionocarbamate byproduct. The topology, thermal and physical properties of the polymer could be altered by adding a difunctional isothiocyanate crosslinker. The synthesis of di and triblock copolymers was possible by using difunctional (macro)initiators and by exploiting the living character of the ROCOP process, which allowed chain-extension by the ring-opening polymerisation (ROP) of lactide. The polymers readily degrade under acidic and basic conditions. Photodegradation without additives is also possible with an 85% decrease in molar mass in one week. The potential of the imidothiocarbonate linkages for metal capture has been investigated, and good affinity for Cu^{2+} ions is seen.

Received 21st April 2023,
Accepted 18th May 2023

DOI: 10.1039/d3py00443k

rsc.li/polymers

Introduction

Sugar derived polymers possess huge potential to combat concerns surrounding petroleum derived plastics.[1–5] Not only are they bio-derived, but they can also impart useful properties such as high thermal stabilities and increased functionality.[6] The addition of sulfur into a polymer chain can also improve the physical and thermal properties of the polymer, such as higher degradation temperatures (T_d) and melting temperature (T_m).[7,8] Sulfur has also been found to introduce interesting properties to a polymer such as the enhancement of electrical and optical characteristics and high affinity to metals.[9,10] The photodegradation of sulfur-containing polymers has also been reported.[11–15]

Ring-opening copolymerisation (ROCOP) can be applied to a diverse array of monomers, incorporating properties from both monomers to selectively produce highly functional polymers.[16,17] Incorporation of sulfur into polymers has been recently reported *via* the ROCOP of isothiocyanates (ITCs) with epoxides, catalysed by Lewis pairs or lithium alkoxide salts, forming exclusively monoimidothiocarbonate linkages.[18–21] Similarly, the ROCOP of ITCs with episulfides, catalysed by bis(triphenylphosphine)iminium chloride (PPNCl), has been shown to selectively form poly(diimidothiocarbonates).[22,23] Recently, LiOBn was applied to sequence selective ring-opening terpolymerisation in which poly(monoimidothiocarbonate) and poly(diimidothiocarbonate) blocks were synthesised with high selectivity.[15,21,24] Although highly active ROCOP of epoxides and ITCs has been achieved with numerous organocatalysts (triethylborane and excess phosphazene base, phosphazenium benzoxide) and organolithium catalysts (*t*-BuOLi and LiOBn), transition metal catalysis is yet to be reported. Furthermore, ROCOP of oxetanes is usually thermodynamically more challenging than with epoxides due to the comparatively low ring strain. To the best of our knowledge, ROCOP between an oxetane and ITCs has not been reported.

Our group, among others, is interested in D-xylose as a promising sustainable feedstock, which can be derived into

[a]*Department of Chemistry, University of Bath, Claverton Down, Bath BA2 7AY, UK. E-mail: a.buchard@bath.ac.uk*
[b]*Materials and Chemical Characterisation Facility (MC^2), University of Bath, UK*
[c]*University of Bath Institute for Sustainability, Bath, UK*

†Electronic supplementary information (ESI) available: Experimental procedures; catalyst screening data; spectroscopic and crystallographic data for **C1**; SEC traces, spectroscopic (NMR, MALDI-ToF MS) and thermal (TGA, DSC) data for the polymers; degradation and metal coordination data. CCDC 2253111. For ESI and crystallographic data in CIF or other electronic format see DOI: https://doi.org/10.1039/d3py00443k

3,5-anhydro-1,2-*O*-isopropylidene-α-D-xylofuranose, **D-Ox**, an oxetane monomer containing a xylofuranose core. Both the cationic and anionic homopolymerisation of **D-Ox** has been reported, with polymers showing excellent thermal properties.[25,26]

The ROCOP of **D-Ox** with heteroallenes, namely, CO_2 and CS_2, as well as cyclic anhydrides has been reported.[27–29] These studies found 1,2-cyclohexanediamino-*N*,*N*-bis(3,5-di-*t*-butylsalicyilidene)-chromium(III), **CrSalen** and PPNCl to be an efficient system to the catalysis the ROCOP of **D-Ox**, however this system has not been applied to ITCs and has been shown to be a poor catalyst for the ROCOP of isocyanates.[30] Recently, Pang and co-workers reported the ROCOP of *p*-tosyl isocyanate using a Mn(III)–Cl salen complex, which allowed for controlled microstructure variation.[31] Herein we have explored the metal catalysed ROCOP of **D-Ox** and ICTs to combine the useful properties of the sugar-based monomers with that of four aromatic ITCs, including di-isothiocyanates used for crosslinking.

Results and discussion

Preliminary experiments

D-ox was prepared from D-xylose in a three-step procedure according to literature and distilled over CaH_2 to give a 77% yield.[29] The copolymerization of **D-Ox** with 3,5-bis(trifluoromethyl)phenyl isothiocyanate (**ITC1**), was first investigated with **CrSalen** and PPNCl (Fig. 1A) (Table S1,† entry 1). This catalyst system has been previously found to be effective in the ROCOP of **D-Ox** with cyclic anhydrides, CO_2 and CS_2, although, to the best of our knowledge, has yet to be reported for the ROCOP of isocyanates and isothiocyanates with epoxides.[29] Polymerizations were initially trialed at $[\textbf{D-Ox}]_0 : [\textbf{ITC}]_0 : [\textbf{CrSalen}]_0 : [\text{PPNCl}]_0$ loadings of 200 : 200 : 1 : 1, at 100 °C, and $[\textbf{D-Ox}]_0$ = 1.52 mol L^{-1} in 1,2-dichlorobenzene (DCB) based on previous literature (Table S1,† entry 1). The appearance of a new broad multiplet at 5.88 ppm in the crude ^{1}H NMR spectrum along with the concomitant decrease of starting material (22% conversion of **D-Ox** after 48 hours), indicated the formation of a ring opened product, which was later confirmed to be the anomeric protons of the polymeric imidothiocarbonate.[29] **CrSalen** was also applied for the first time to the ROCOP of cyclohexene oxide (CHO) and **ITC1**; the crude ^{1}H NMR spectrum showed full conversion of CHO to the polyimidothiocarbonate in agreement with reported spectra (Table S1,† entry 2).[19]

Product characterisation

The crude ^{1}H NMR spectrum showed novel major and minor multiplets in the anomeric region at 5.88 and 6.12 ppm respectively, with diffusion ordered spectroscopy (DOSY) NMR spectroscopy showing diffusion coefficients of 1.21×10^{-10} and 8.01×10^{-10} m^2 s^{-1} respectively, confirming the formation of two main species (Fig. 1C and S13†). The major product was precipitated selectively from cold methanol and size-exclusion-chromatography (SEC; against narrow polystyrene standards) analysis of the isolated product confirmed the polymeric nature of the product ($M_{n,SEC}$ = 7000 g mol^{-1}. ^{1}H NMR spec-

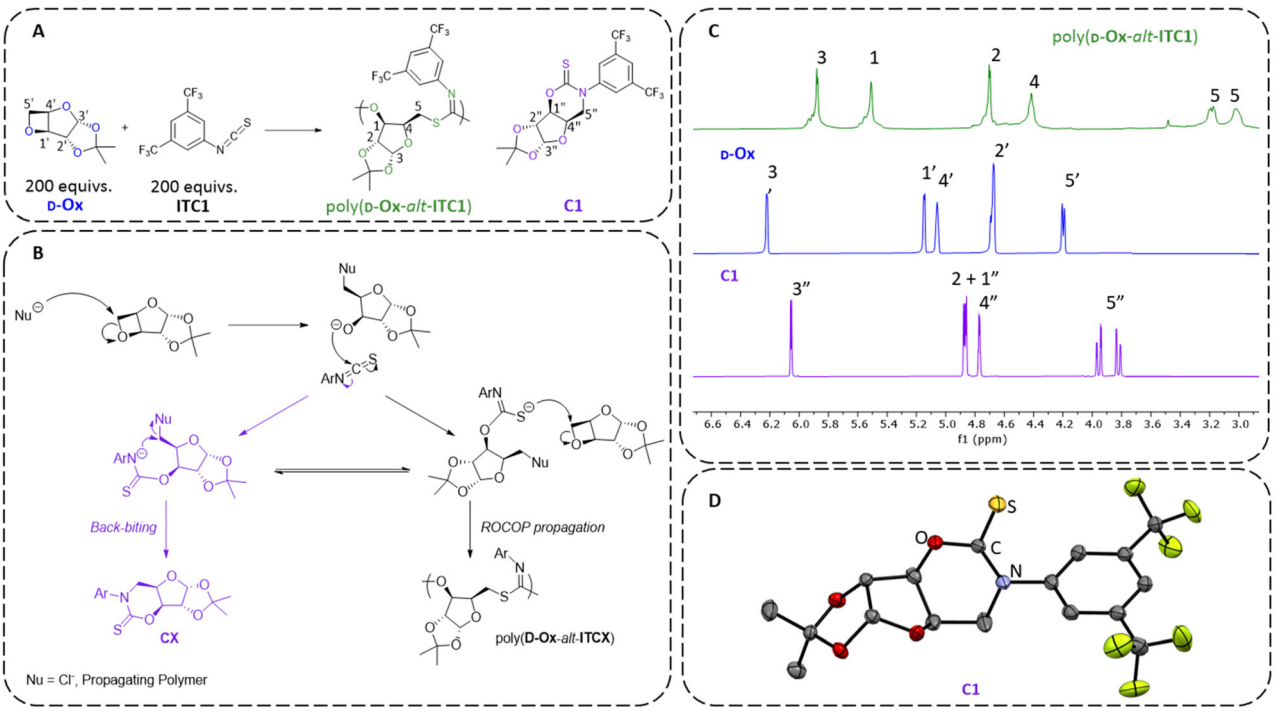

Fig. 1 (A) Scheme for the copolymerization of **D-Ox** and **ITC1**. (B) Suggested routes towards formation of **C*X*** and poly(**D-Ox**-*alt*-**ITC*X***). (C) ^{1}H NMR spectra (500 MHz, $CDCl_3$) of isolated poly(**D-Ox**-*alt*-**ITC1**), **D-Ox** and isolated **C1**. (D) Crystal structure of **C1**.

troscopy showed an equal ratio of D-Ox and **ITC1** incorporated in the polymer chain, suggesting the expected alternating copolymer species, and confirmed by MALDI ToF spectrometry (Fig. S1 and S11† respectively).

Selective imidothiocarbonate formation was confirmed by the presence of only one resonance at 158 ppm in the ^{13}C NMR spectrum and a strong band at 1632 cm^{-1} in the Fourier-transform infrared (FTIR) spectrum (Fig. S2 and S6†).[19] The single imine resonance also indicated consistent regioselective opening of D-Ox by the propagating sulfur anion. The alternative thionocarbamate linkage was not observed within the limit of NMR and IR spectroscopy in agreement with the work of Song and co-workers.[19] ^{1}H–^{13}C heteronuclear multiple bond correlation (HMBC) NMR spectroscopy showed correlation between the imine resonance and the xylofuranose component in exclusively the **3** and **5** positions indicating selective opening of D-Ox across the oxetane moiety (Fig. S4†).

The side product (**C1**) was isolated by precipitation from hexane from a solution of side product and monomer mix, with single crystals of **C1** isolated from hexane and chloroform in a 5 : 1 ratio. In contrast to the polymer, a single resonance in the ^{13}C NMR spectrum at 186 ppm confirmed complete formation of the cyclic thionocarbamate (Fig. S17†). This was supported by X-ray diffraction data of single crystals of **C1** (Fig. 1D).

Catalyst screening

Aluminium and iron amino-tris(phenolate) (**AlTris** and **FeTris**) complexes were applied to the ROCOP of D-Ox with **ITC1** due to their reported success in the ROCOP of epoxides and cyclic anhydrides where one of the monomers is sterically encumbered.[32–34] Both complexes were found to greatly increase the rate of copolymerisation with D-Ox. A conversion of 84% of D-Ox could be achieved with **AlTris** in 6 hours with SEC showing molar masses ($M_{n,SEC}$) up to 21 300 g mol^{-1} and a moderate dispersity ($Đ_M$) of 1.63 (Table 1, entry 1). The crude ^{1}H NMR spectrum showed that only 2% of converted D-Ox formed **C1**, the rest being polymer. With **FeTris**, 85% conversion of D-Ox was achieved after 6 hours, 6% being **C1**, which likely resulted in lower molar mass polymers ($M_{n,SEC}$ = 15 900 g mol^{-1}, $Đ_M$ = 1.62, Table S1,† entry 7).

When altering the ligand structure from an amino tris(phenolate) ligand to a porphyrin ligand, the catalyst selectivity switched towards formation of **C1**. Under identical conditions an aluminium porphyrin (**AlPorph**) complex was tested with PPNCl. After 6 hours, 56% conversion of D-Ox was observed; 7% of the D-Ox had converted to polymer whereas 49% had converted to **C1** (Table S1,† entry 9). After 48 hours, 80% of overall species were side products (Table S1,† entry 8). Polymers isolated from methanol showed low molar masses ($M_{n,SEC}$ = 4000 g mol^{-1}).

Optimisation and control

Building from the high reactivity and selectivity of the **AlTris** complex, optimisation of the reaction was done to minimise the formation of side products. Polymerisation at 100 °C in the absence of solvent resulted in the solidification of the reaction mixture which limited monomer conversion (95% *vs.* >99% in solution; Table S2,† entry 3), although $M_{n,SEC}$ of 20 000 g mol^{-1} could still be achieved (Table 1, entry 2). The temperature was then reduced with the aim of decreasing the production of **C1**. At 80 °C in DCB, polymer selectivity was 95% (detected by ^{1}H NMR spectroscopy) (Table 1, entry 3). Toluene and acetonitrile were then trialed to minimise the use of halogenated solvents and high polymerisation selectivity was maintained (Table 1, entries 4 and 5). Further reduction in temperature to 60 °C resulted in no detection of **C1** by ^{1}H NMR spectroscopy but much reduced conversions (Table 1, entries 6 and

Table 1 Optimisation of the ROCOP of D-Ox and ITC1

Entry	Catalyst[a]	Temp (° C)	D-Ox : AlTris	Solvent	$[D\text{-Ox}]_0$ (mol L^{-1})	Time (h)	Conv.[b] (%)	Polymer select.[c] %	$M_{n,theo}$[d]	$M_{n,SEC}$[e] ($Đ_M$)
1	**AlTris**	100	200 : 1	DCB	1.52	6	84	98	72 700	21 300 (1.63)
2	**AlTris**	100	200 : 1	None	3.03	48	95	92	77 100	20 000 (1.64)
3	**AlTris**	80	200 : 1	DCB	1.52	24	97	95	81 500	22 300 (1.40)
4	**AlTris**	80	200 : 1	Toluene	1.52	24	>99	97	86 000	22 000 (1.62)
5	**AlTris**	80	200 : 1	Acetonitrile	1.52	24	95	96	80 700	28 000 (1.50)
6	**AlTris**	60	200 : 1	Toluene	1.52	6	21	95	17 800	12 700 (1.17)
7	**AlTris**	60	200 : 1	Toluene	1.52	24	60	>99	53 200	24 300 (1.41)
8	**AlTris**	80	200 : 1	Toluene	1.00	6	27	96	24 000	14 000 (1.22)
9	**AlTris**	80	200 : 1	Toluene	1.00	24	74	99	64 700	28 200 (1.44)
10	**AlTris**[f]	80	200 : 1	Toluene	1.52	24	<1	<1	<1000	<1000
11	**None**	80	200 : 1	Toluene	1.52	24	<1	<1	<1000	<1000
12	**None**[f]	80	200 : 1	Toluene	1.52	24	<1	<1	<1000	<1000
13	**AlTris**	80	300 : 1	Toluene	1.52	48	92	89	109 000	28 700 (1.62)
14	**AlTris**	80	400 : 1	Toluene	1.52	48	83	98	143 600	34 900 (1.71)
15	**AlTris**	80	500 : 1	Toluene	1.52	48	23	96	48 800	20 500 (1.30)

[a] Reactions carried out at $[D\text{-Ox}]_0$ = 1.52 mol L^{-1} with a 200 : 200 : 1 : 1 ratio of D-Ox : ITC1 : AlTris : PPNCl unless otherwise stated. [b] Conversion of D-Ox determined by ^{1}H NMR spectroscopy by relative integration of anomeric protons in D-Ox ($CDCl_3$, δ = 6.26 ppm (d, J = 3.7 Hz)) and poly(D-Ox-*alt*-ITC1) ($CDCl_3$, δ = 5.81 ppm (m)). [c] Percentage of converted D-Ox to poly(D-Ox-*alt*-ITC1). [d] Calculated as $M_r(Cl) + ((M_r(D\text{-Ox}) + M_r(ITC1)) \times [D\text{-Ox}]_0/[PPNCl]_0 \times \%\ conv./100)$. [e] Calculated by SEC relative to polystyrene standards in THF eluent, $Đ_M = M_w/M_n$. [f] Reactions carried out without PPNCl.

7). Reducing the initial concentration of D-Ox to 1.0 mol L^{-1} at 80 °C resulted in reduced rates too, but with no significant improvement in selectivity (Table 1, entries 8 and 9). Control experiments showed that without the simultaneous presence of both **AlTris** and PPNCl no polymerisation was observed (Table 1, entries 10–12).

The **D-Ox : AlTris** ratios were then decreased to 300 : 1, 400 : 1 and 500 : 1, keeping $[\text{D-Ox}]_0$ constant, with the aim of synthesising high molar mass polymers (Table 1, entries 13, 14 and 15 respectively). The rate was significantly affected by lowering the catalyst concentration and full conversion was not achieved after 48 hours at any low loading of catalyst. However, higher molar mass polymers were still obtained at ratios of 300 : 1 and 400 : 1 ($M_{n,SEC}$ = 28 700 and 34 900 g mol^{-1} respectively), although at 500 : 1 the negative effect of impurities was too great to achieve high molar mass polymers.

To demonstrate the living character of the ROCOP process, a sequence addition experiment was performed. Reactions were initially carried out at 80 °C in toluene with 0.25 mmol of **D-Ox** and **ITC1** (**D-Ox : ITC1 : AlTris** : PPNCl loadings of 50 : 50 : 1 : 1) and monitored by ^{1}H NMR spectroscopy and SEC. After 24 hours the conversion of **D-Ox** was >99% and an additional 1 mmol of **D-Ox** and **ITC1** were added. A conversion of >99% was achieved after 24 hours. An increase in the molar mass was observed upon addition of the second batch of monomers ($M_{n,SEC}$ before second monomer batch addition = 7600 g mol^{-1}, $Đ_M$ = 1.47; $M_{n,SEC}$ after second monomer batch addition = 13 300 g mol^{-1}, $Đ_M$ = 1.56, Fig. S14†). ^{1}H DOSY NMR spectroscopy of the polymer showed a single diffusion coefficient (1.11 × 10^{-11} m^2 s^{-1}, Fig. S15†) for all resonances associated with poly(**D-Ox**-*alt*-**ITC1**), consistent with chain extension, albeit to a lesser degree than expected (likely from the introduction of additional chain transfer agent impurities (*vide infra*)).

Plots of conversion against $M_{n(SEC)}$ and $Đ_M$ showed a linear increase in $M_{n(SEC)}$ against **D-Ox** conversion (Fig. S12†). At intermediate conversions, SEC analysis showed bimodal distributions leading to higher dispersities, probably from concurrent initiation by chloride anions and by diprotic impurities in **D-Ox**, as typically observed in ROCOP. MALDI-ToF mass spectrometry corroborated this as three polymer series were detected (Fig. S11†) with repeat units of 443 g mol^{-1}. The presence of residual protic impurities, acting as chain transfer agents, also meant that despite the living nature of the ROCOP, $M_{n,SEC}$ values were consistently lower than theoretical ones ($M_{n,theo}$) (*e.g.*, for Table S1†, entry 3 $M_{n,theo}$ = 55 000 g mol^{-1} *vs.* $M_{n,SEC}$ = 21 000 g mol^{-1}).

Optimisation towards formation of C1 and reactivity

Using the aluminium porphyrin complex **AlPorph,** the reaction selectivity could be altered to form 100% of **C1**, with no sign of polymer or monomer in the ^{1}H crude NMR spectrum. This was achieved at 120 °C, at **D-Ox : ITC1 : AlPorph** : PPNCl loadings of 100 : 100 : 1 : 1 in DCB. A suggested mechanism is shown in Fig. 1B. Compared to **AlTris**, the porphyrin ligand clearly influences the relative energy barrier between the propagation and back-biting steps. Selectivity towards thionocarbamate formation over the imidothiocarbonate during backbiting was attributed to greater stability of the nitrogen anion, which may also be enhanced by the porphyrin ligand system.

ROP of **C1** was attempted with KO^{t}Bu and 18-crown-6-ether at 120 °C (**D-Ox : ITC1** : KO^{t}Bu : 18-crown-6-ether loadings of 100 : 00 : 1 : 1) and with **AlTris** and PPNCl at 80 °C (**D-Ox : ITC1 : AlTris** : PPNCl loadings of 100 : 100 : 1 : 1). After 24 hours under both conditions, no polymeric species was detected by SEC and the crude ^{1}H NMR spectra showed no change to **C1**. The lack of reactivity of **C1** under identical conditions to that of **D-Ox**/**ITC1** ROCOP indicates the formation of **C1** is irreversible and therefore not likely to be an intermediate in the polymerisation. Without closer reaction monitoring, it is however unclear at this stage if any propagation happens before back-biting or if back-biting occurs straight after initiation.

Kinetic studies

To gain a deeper understanding of reaction kinetics, [**D-Ox**] *vs.* time data were acquired using *in situ* FTIR spectroscopy by analysing the decrease in the absorption intensity at 1087 cm^{-1} corresponding to a ν_{C-O} vibration in **D-Ox**. The catalyst and cocatalyst were used in a 1 : 1 ratio and varied simultaneously. The reaction rate was evaluated for [**AlTris**–PPNCl] = 15 and 20 mmol L^{-1}, using a 1.12 mol L^{-1} concentration of **D-Ox** in toluene at 80 °C, with triethylsilane as an internal standard for offline NMR analysis.

Visual kinetic analysis developed by Burés and co-workers revealed a second order dependence with respect to [**AlTris**–PPNCl] (Fig. 2A).[35] It may be that the catalyst and co-catalyst both have an order of one and work in tandem: **AlTris** activating the monomer and **PPNCl** stabilising the anion. Alternatively, non-covalent dimeric aluminium species may be formed *in situ* as reported in the literature.[36] A more in-depth kinetic analysis would be required to delineate the role of each component of this binary catalytic system.

Semi-logarithmic plots of ln([**D-Ox**]) against time from 0–75% conversion showed linear fits indicative of a first-order dependence on **D-Ox** concentration. At a catalyst loading of 20 mmol L^{-1} k_{obs} was found to be 3.18 (±0.01) × 10^{-4} s^{-1} (Fig. 2B) These results suggests that the rate determining step is the ring-opening of the oxetane. The formation of **C1** was not detectable by *in situ* FTIR spectroscopy or in the final crude ^{1}H NMR spectrum, and a direct correlation between polymer production and **D-Ox** consumption was observed with no induction period.

Expanding the monomer scope

The procedure was then extended to a range of aliphatic and aromatic isocyanates with **AlTris**. ROCOP with aliphatic isocyanate, isopropyl isothiocyanate (**ITC2**) yielded no detectable polymeric species after 24 hours and only oligomeric species after 72 hours (Table 2, entries 1 and 2). 2-Chloroethyl isothio-

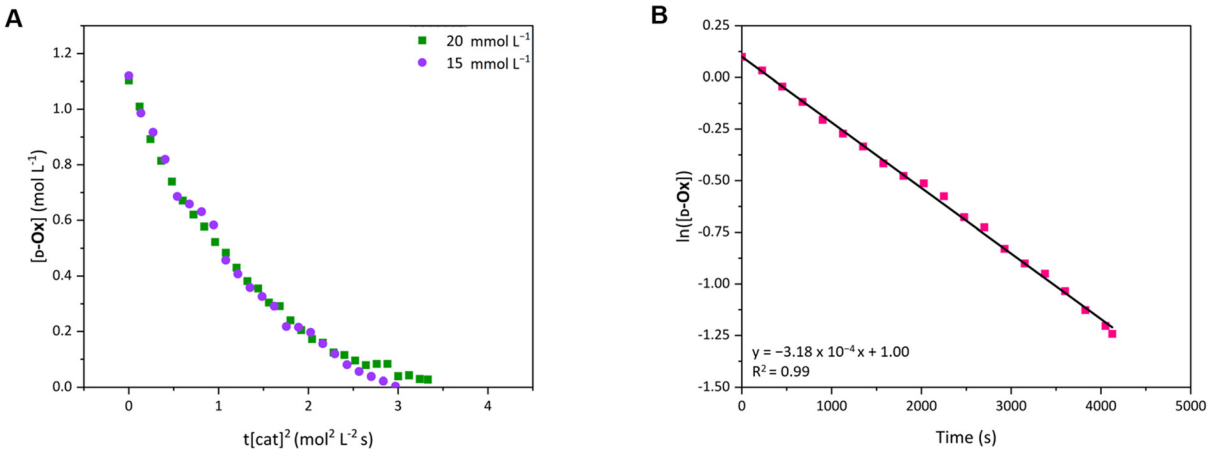

Fig. 2 Kinetic data acquired by *in situ* FTIR spectroscopy, varying catalyst loading, [D-**Ox**] = 1.12 mol L^{-1} at 80 °C in toluene. (A) Visual kinetic analysis plot of normalised time against [D-**Ox**] at [cat] = [**AlTris**–PPNCl] = 20 and 15 mmol L^{-1}. (B) Logarithmic plot of [D-**Ox**] *vs*. time from 0–75% conversion of D-**Ox**, [**AlTris**–PPNCl] = 20 mmol L^{-1}.

cyanate (**ITC3**), produced entirely the cyclic back-biting product, **C3**.

For all aromatic substrates tested, alternating AB copolymers were primarily synthesised. ROCOP with phenyl isothiocyanate (**ITC4**) and *p*-tolyl isothiocyanate (**ITC5**) proceeded with considerably lower conversions compared with **ITC1** (conversion after 24 hours was 41 and 44% compared to >99% respectively), indicating the electron withdrawing groups significantly enhance the reactivity of the isothiocyanate towards ROCOP with D-**Ox** (Table 2, entries 5–8).

Poly(D-**Ox**-*alt*-**ITC4**) and poly(D-**Ox**-*alt*-**ITC5**) could be isolated with $M_{n,SEC}$ up to 9100 and 4600 g mol^{-1} respectively, with any conversion of D-**Ox** after 24 hours mostly being converted to **C4**/**5**. This switch in catalyst regime to favour polymerisation with aromatic substrates *versus* aliphatic suggests the aromatic substituent has a part in directing catalysis towards ROCOP. We propose that aliphatic substituents increase the nucleophilicity of the nitrogen atom, favouring thionocarbamate formation which results in cyclisation (see suggested mechanism, Fig. 1B).

Phenyl diisothiocyanate (**ITC6**) was added to ROCOP of D-**Ox** with **ITC4** (2.5–50% **ITC6** in **ITC4**) to form crosslinked polymers. SEC analysis of the isolated polymers showed broad traces typical of crosslinked polymers. Due to signal overlapping in the aromatic region, ^{1}H NMR analysis could not be used to quantify the incorporation of cross-linker. However, as the **ITC6** loading was increased, new signals in the ^{13}C NMR in the aromatic region at 126.6 and 122.5 ppm were observed confirming incorporation of **ITC6** into the polymer chain (Fig. S28†). Increasing the crosslinking (**ITC6** >10%), resulted in solidification of the reaction mixture, presumably limiting conversion although NMR and SEC analysis was not possible due to insolubility.

Thermal analysis

Thermal analysis of poly(D-**Ox**-*alt*-**ITC1**) with a range of molar masses between 11 300 and 26 200 g mol^{-1} was undertaken to understand the impact of molar mass on the properties.[25] All polymers analysed were found to have glass transition temperatures (T_g) between 106 to 117 °C, with increased molar mass resulting in increased T_g (Fig. S10†). Temperatures of onset of degradation ($T_{d,5\%}$) were found to be between 228 to 269 °C. These are higher than polyimidothiocarbonates synthesised from epoxide ROCOP with ITCs reported by Feng and co-workers (max T_d 220 °C).[20] This is likely due to the furanose ring, which has been previously found to improve the thermal stability of polymers.[29] Mass spectrometry detected species during the primary degradation step with m/z = 44 and 55, which were attributed to S–C and C–N=C–O ions, indicating that the thermal break down of the imidothiocarbonate linkages occurs first (Fig. S9†). A small, secondary degradation step at higher temperatures was observed for all TGA with mass spectrometry of the degradation products showing species with m/z = 81 and 96. This is likely a secondary degradation of the furanose core.

Poly(D-**Ox**-*alt*-**ITC4**) showed similar thermal properties; however poly(D-**Ox**-*alt*-**ITC5**) possessed a markedly lower T_g, likely due to a combination of low molar mass and reduced polarity. As expected, thermal analysis of the crosslinked polymers showed high T_gs, increasing with crosslinking density, as well as multiple thermal degradation steps indicative of varied chain linkages, with higher crosslinking densities resulting in greater residual char (Fig. S29†).[25]

Hydrolytic and UV degradation

An attractive feature of sugar derived polymers is the high content of polarised bonds resulting in multiple sites for the degradation of the polymer backbone. It was envisioned that the imidothiocarbonate linkages would be susceptible to hydrolysis under both acidic and basic conditions. Poly(D-**Ox**-*alt*-**ITC1**) was thus stirred in a 1 mol L^{-1} $HCl_{(aq)}$ THF mixture at 50 °C and a rapid decrease in polymer molar mass was observed (by 85% within 5 hours, Fig. 3). Identification of the degradation products by ^{1}H and ^{13}C NMR spectroscopy proved

Table 2 ROCOP of D-Ox with various ITCs

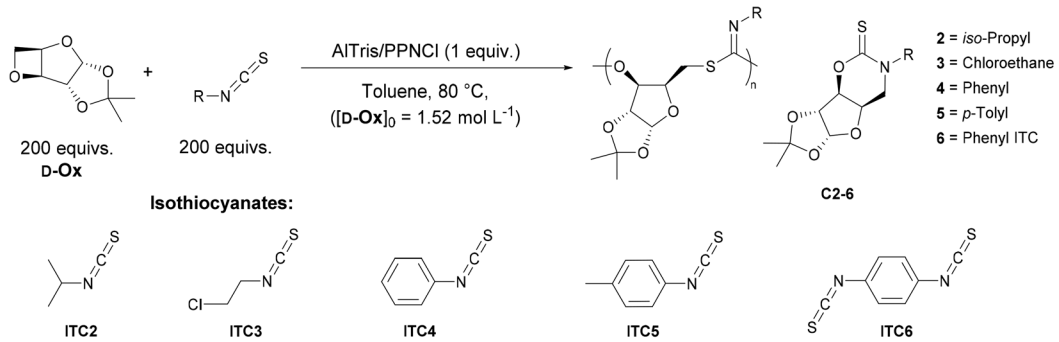

Entry	Comonomer (ITC ratio)[a]	Time (h)	Conv.[b] (%)	Polymer select.[c] (%)	$M_{n,theo}$ [d]	$M_{n,SEC}$ [e]	$Đ_M$ [e]	T_g [f] (°C)	$T_{d,5\%}$ (°C)
1	**ITC2**	24	2	>99	1100	<1000	—	—	—
2	**ITC2**	72	17	94	8800	1700	1.06	—	—
3	**ITC3**	24	62	0	<1000	<1000	—	—	—
4	**ITC3**	72	81	0	<1000	<1000	—	—	—
5	**ITC4**	24	41	95	24 000	6600	1.50	111	264
6	**ITC4**	72	84	62	38 100	9100	1.59	109	248
7	**ITC5**	24	40	74	21 900	4600	1.15	75	228
8	**ITC5**	72	61	62	24 400	4400	1.12	80	237
9	**ITC6 : ITC4** (2.5 : 97.5)	72	50	90	30 800	9200	2.10	105	274
10	**ITC6 : ITC4** (5 : 95)	72	29	93	16 600	29 100	2.41	108	273
11	**ITC6:ITC4** (7.5 : 92.5)	72	61	84	31 400	11 300	3.91	116	261
12	**ITC6 : ITC4** (10 : 90)	72	72	85	37 600	—	—	132	267
13	**ITC6 : ITC4** (20 : 80)	72	—	—	—	—		134	175
14	**ITC6 : ITC4** (50 : 50)	72	—	—	—	—		129	208

Reactions carried out at $[D\text{-}Ox]_0$ = 1.52 mol L^{-1} in toluene with a 200 : 200 : 1 : 1 ratio of D-Ox : ITC : **AlTris** : **PPNCl** at 80 °C unless otherwise stated, reaction quenched when stirring stopped. [a] Ratio of moles of specified ITC. [b] Conversion of D-Ox determined by ^{1}H NMR spectroscopy by relative integration of anomeric protons in D-Ox ($CDCl_3$, δ = 6.26 ppm (d, J = 3.7 Hz)) and poly(D-Ox-*alt*-**ITC*X***) ($CDCl_3$, δ = 6.03–5.81 ppm (m)). [c] Percentage of converted D-Ox to poly(D-Ox-*alt*-**ITC*X***). [d] (Calculated as M_r(Cl) + ((M_r(D-Ox) + M_r(**ITC*X***)) × $[D\text{-}Ox]_0$/$[PPNCl]_0$ × % conv./100). [e] Calculated by SEC relative to polystyrene standards in THF eluent, $Đ_M = M_w/M_n$. [f] Values taken from second heating cycle.

challenging (Fig. S30 and S31†). Further analysis of the degradation products after 3 hours by ^{19}F NMR spectroscopy was also inconclusive, albeit a new signal appearing downfield to that of the polymer (−62.8 *vs.* −63.1 ppm, respectively) (Fig. S32†).

The polymer was also stirred in THF and $NaOH_{(aq)}$ at a 1 mol L^{-1} concentration at 50 °C: after 30 min no polymeric species was detected by SEC analysis (Fig. 3). Analysis of the degradation products by mass spectroscopy detected a major species of a molar mass of 444.07 g mol^{-1}, the mass of the repeat unit and an additional proton, suggesting formation of a cyclic product (Scheme 1 and Fig. S38†). In the ^{13}C NMR spectrum (Fig. S35†), the presence of an imine resonance at 159 ppm indicated the formation of a cyclic imidothiocarbonate, with the HMBC spectrum confirming coupling between the imine group and the xylofuranose moiety (Fig. S37†). A suggested mechanism for the basic degradation and back-biting towards the cyclic imidothiocarbonate product is shown on Scheme 1. Notably such back-biting and that seen during the ROCOP process proceeds from different chain-ends (alkoxide and carbamate, respectively), resulting in two different structural isomers.

Our group, among others, has also recently reported photodegradation of sulfur containing polymers.[12] Upon UV radiation at 365 nm for 5 hours without any additives in THF, the M_n of poly(D-Ox-*alt*-**ITC1**) decreased by 10%.[12] After 24 hours and 1 week, the M_n had decreased by 20% and 85% respectively (Fig. 3). When stirred in the dark, the M_n of poly(D-Ox-*alt*-**ITC1**) did not decrease. Poly(D-Ox-*alt*-**ITC1**) also showed good

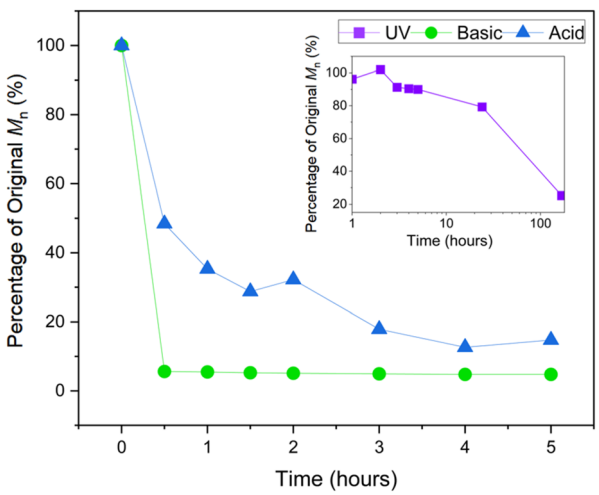

Fig. 3 Degradation plots of poly(D-Ox-*alt*-**ITC1**) ($M_{n,SEC}$ = 21 800 g mol^{-1}, $Đ_M$ = 1.33). Photodegradation conducted in THF exposed to 365 nm radiation. Basic and acidic degradation done in THF with aqueous NaOH and HCl respectively (1 mol L^{-1}) at 50 °C.

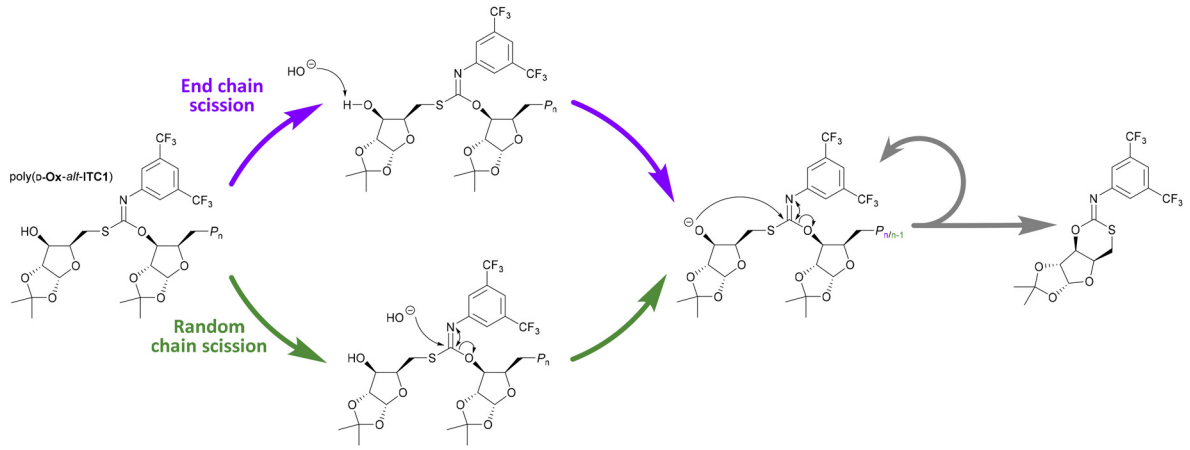

Scheme 1 Two proposed pathways for basic degradation of poly(D-**Ox**-*alt*-**ITC1**).

thermal stability when stirred at 140 °C in tetrachloroethane, with no cyclic species detected by ^{1}H NMR spectroscopy.

Polymer architecture variations

To synthesise more complex polymer architectures, initiating systems other than chloride anions (from PPNCl) were investigated under the identified standard ROCOP conditions (80 °C, $[$D-**Ox**$]_0$ = 1.52 mol L^{-1} in toluene). Initial experiments with 1,8-diazobicyloco[5.4.0]undec-7-ene (DBU) and **AlTris** were undertaken. It was hypothesised that in the presence of a base, residual protic species in the monomer (specifically 1,2-*O*-isopropylidene-xylofuranose or IPXF) would form alkoxide species able in turn to initiate D-**Ox** ROCOP. At a **AlTris** : DBU : D-**Ox** : **ITC1** ratio of 1 : 1 : 200 : 200, low dispersity poly(D-**Ox**-*alt*-**ITC1**) with moderate M_n was isolated (M_n = 6600 g mol^{-1} $Đ_M$ = 1.13). Having established that initiation from protic impurities in the monomer was possible, an exogeneous alcohol initiator was next purposedly added.

Experiments with 1,4-butanediol (BD) as the initiator were undertaken at a BD : **AlTris** : DBU : D-**Ox** : **ITC1** ratio of 1 : 2 : 2 : 40 : 40 (Fig. 4Ai). The crude ^{1}H NMR spectrum showed 70% selectivity towards the polymer (Table S2,† entry 1). ^{1}H NMR analysis of the isolated polymer revealed two new signals at 4.14 and 1.95 ppm which were attributed to BD incorporations into the polymer ($M_{n,SEC}$ = 8400 g mol^{-1}, $Đ_M$ = 1.20) (Fig. S40†). However, DOSY NMR spectroscopy showed two main diffusion coefficients for signals assigned to the polymer, likely due to initiation from both monomer protic impurities and BD (Fig. S41†). The initiating groups could not be assigned with MALDI ToF mass spectrometry although the repeating unit of 443 was observed (Fig. S42†).

The ratio of D-**Ox** : BD was then increased with the aim of making higher M_n polymers (Table S2,† entries 2–5). The molar mass increased with decreasing initiator loading up to 11 000 g mol^{-1} at a BD : **AlTris** : DBU : D-**Ox** : **ITC1** ratio of 1 : 2 : 2 : 200 : 200. Further decrease in initiator loading had no effect on molar masses, which was attributed to residual protic impurities outcompeting the BD as the predominating initiators.

To demonstrate the potential of the alcohol initiated ROCOP of D-**Ox**, initiation from a diol capped polymer was then attempted. Polyethylene glycol (PEG) was chosen as the bifunctional macroinitiator due to its simple structure and low T_g, a desirable property in the synthesis of ABA triblock copolymers for thermoplastic elastomers (Fig. 4Aii). ROCOP was carried out with commercial PEG with a molar mass of 6000 g mol^{-1} at a PEG : **AlTris** : DBU : D-**Ox** : **ITC1** ratio of 1 : 2 : 2 : 100 : 100. Crude ^{1}H NMR analysis showed a 91% conversion of D-**Ox**, with 85% selectivity towards poly(D-**Ox**-*alt*-**ITC1**). As anticipated, ^{1}H NMR analysis of the isolated polymer showed it contained PEG, with a single resonance at 3.64 ppm (Fig. S43†). The crude SEC trace was bimodal which was attributed to the presence of two initiating species: the low molar mass species initiated from protic small molecule impurities (water or IPXF) and high molar mass species initiated by chain extension from PEG ($M_{n,SEC}$ of PEG = 11 000 g mol^{-1}, $Đ_M$ = 1.14; $M_{n,SEC}$ after chain extension = 19 400 g mol^{-1}, $Đ_M$ = 1.08) (Fig. 4Bi). This was confirmed with DOSY NMR which showed one species diffusing at 6.36 × 10^{-10} m^2 s^{-1} (Fig. S44†). Chain extension of PEG with poly(D-**Ox**-*alt*-**ITC1**), lowered the T_m from 63 °C to 47 °C, determined by DSC, and only one T_g at −29 °C was observed, indicating no microphase separation between PEG and poly(D-**Ox**-*alt*-**ITC1**), likely due to short copolymer blocks (Fig. S45†).

Next, the synthesis of ABA-type triblock copolymers with poly L-lactic acid (PLLA) blocks was investigated. First, sequential addition of L-lactide to poly(D-**Ox**-*alt*-**ITC1**) was attempted (Fig. 4Aiii). The poly(D-**Ox**-*alt*-**ITC1**) block was synthesised under standard conditions with BD and DBU as the initiating system (BD : **AlTris** : DBU : D-**Ox** : **ITC1** loadings of 1 : 2 : 2 : 50 : 50) and monitored by ^{1}H NMR spectroscopy and SEC. After 18 hours the conversion of D-**Ox** was >99% and 200 equivalents of L-lactide was then added. The reaction was quenched after 24 hours and crude ^{1}H NMR spectroscopy showed 94% conversion of L-lactide to PLLA. DOSY NMR of the isolated polymer showed a single diffusion coefficient at 7.76 × 10^{-11} m^2 s^{-1} (Fig. S48†) and confirmed formation of a

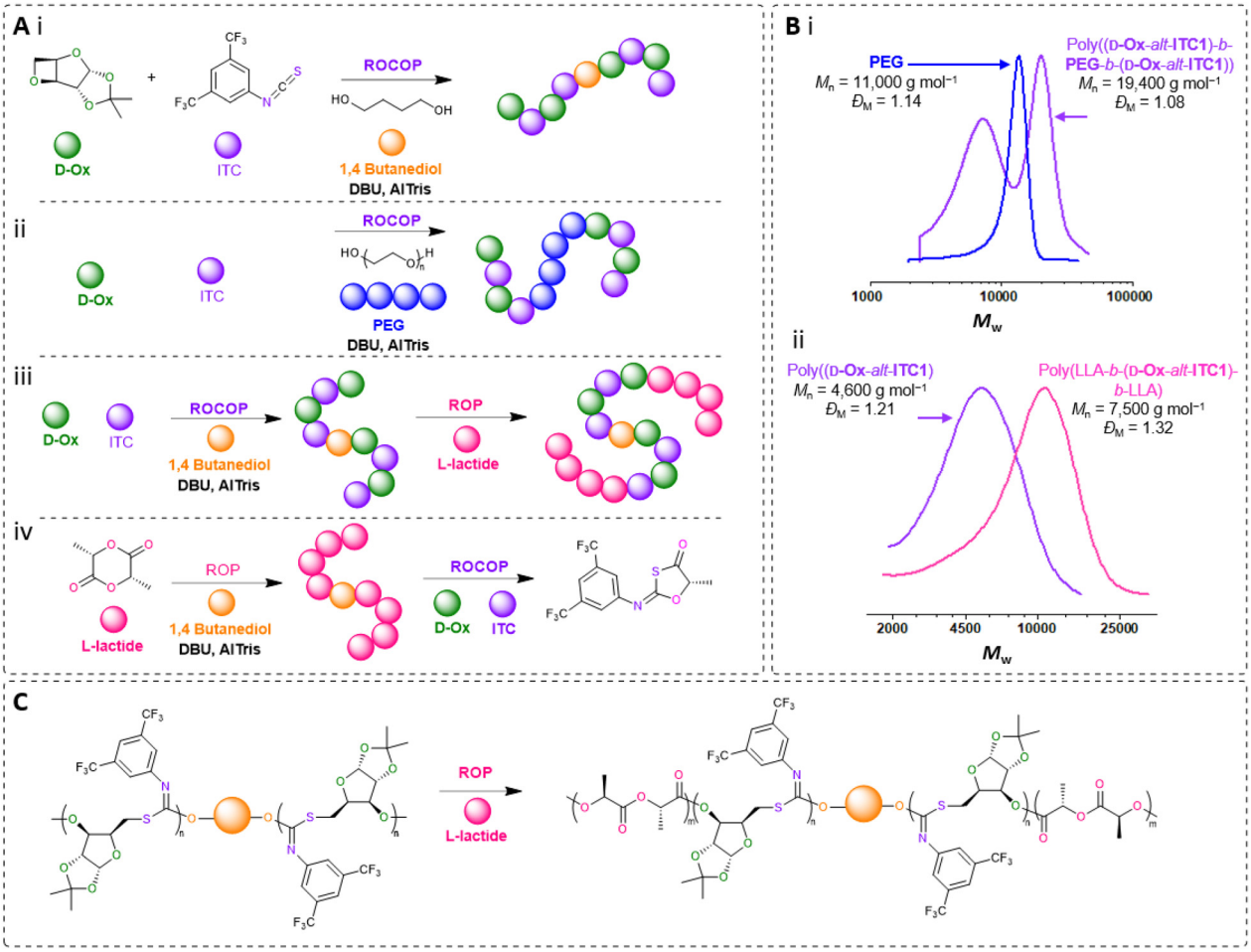

Fig. 4 (A) (i) Schematic of D-**Ox** and **ITC1** ROCOP initiated by BD in the presence of DBU, (ii) schematic of D-**Ox** and **ITC1** ROCOP initiated by PEG under basic conditions, (iii) schematic of D-**Ox** and **ITC1** ROCOP initiated by BD under basic conditions followed by chain extension by ROP of L-lactide, (iv) schematic of the synthesis of IMOT from PLA, D-**Ox** and **ITC1**. (B) (i) SEC traces of commercial PEG and an aliquot taken after ROCOP with D-**Ox** and **ITC1** (in chloroform), (ii) SEC traces of an aliquots taken after ROCOP with D-**Ox** and **ITC1** and chain extension by ROP of L-lactide. (C) The polymer structure of poly(LLA-*b*-(D-**Ox**-*alt*-**ITC1**)-*b*-LLA).

true PLLA-poly(D-**Ox**-*alt*-**ITC1**) copolymer. An increase in the molar mass was also observed ($M_{n,SEC}$ 4600 g mol^{-1} ($Đ_M$ = 1.21) before L-lactide addition; $M_{n,SEC}$ 7500 g mol^{-1} ($Đ_M$ = 1.32) after LA ROP; Fig. 4Bii). ^{1}H NMR analysis of the isolated block copolymer showed some broadening of the PLLA quartet at 5.16 ppm and the anomeric proton resonance at 5.88 ppm, which was attributed to chain scrambling occurring (Fig. S46†).

This was confirmed by the appearance of new signals between 175.21–169.36 ppm in the ^{13}C NMR spectrum, confirming the formation of new carbonyl linkages (Fig. S47†). DSC analysis showed a single T_g (41 °C), lower than both PLA and poly(D-**Ox**-*alt*-**ITC1**) (Fig. S49†). This has been attributed to chain scrambling resulting in small blocks which inhibit polymer chain stacking.

Surprisingly, the synthesis of poly((D-**Ox**-*alt*-**ITC1**)-*b*-LLA-*b*-(D-**Ox**-*alt*-**ITC1**)) by addition of D-**Ox** and **ITC1** to a telechelic PLLA macroinitiator, resulted in complete degradation of PLLA and no new polymeric species detected by SEC (Fig. 4Aiv). ((3,5-Bis(trifluoromethyl)phenyl)imino)-5-methyl-1,3-oxathiolan-4-one was isolated *via* sublimation and the structure was confirmed by NMR spectroscopy. ^{13}C NMR analysis showed one carbonyl and imine peak at 172 and 154 ppm respectively and the HMBC spectrum showed correlation between the imine resonance and the methine at 5.07 ppm (Fig. 4Aiii and Figs. S51, S54†). It is worth noting that this oxathiolane does not incorporate any xylose moiety. A suggested mechanism, relying on ICT insertion, transesterification and back-biting steps, is shown in the ESI (Scheme S1†).

Metal coordination

The high functional group content of poly(D-**Ox**-*alt*-**ITC1**) prompted us to preliminarily assess its performance as metal ion absorbent. It was hypothesised that the imidothiocarbonate linkage could act as a coordinating group. Indeed, previous studies have found S and N containing polymers to be effective at removal of Hg^{2+} from aqueous solutions, with adsorption of Hg^{2+} often attributed to simultaneous binding

to S and N.[37–39] Similarly, polymeric Schiff bases have been found to form metal complexes, in particular with Cu^{2+}.[40–46]

Two metal ions were considered, Cu^{2+} and Co^{3+}, which had been previously identified as toxic metals found in wastewater and which would allow colorimetric titration to monitor complexation.[47] Initial tests with 0.1 mol L^{-1} $[Co(NH_3)_6]Cl_3$ and $Cu(OAc)_2{\cdot}H_2O$ in water with poly(D-**Ox**-*alt*-**ITC1**) at 80 °C were carried out. Poly(D-**Ox**-*alt*-**ITC1**) remained insoluble in water at 80 °C with stirring. After 24 hours, each polymer was washed with water and centrifuged, until the supernatant was colourless, and dried *in vacuo* at 50 °C.

Polymers exposed to Cu^{2+} and Co^{3+} (polymer-Cu and polymer-Co respectively) were not soluble in common NMR solvents. After exposure to metal ions, polymer-Cu showed greater absorbance by FTIR spectroscopy at 1627 cm^{-1} and 1431 cm^{-1}, corresponding to C=N and S–C stretches respectively, and was therefore investigated further (Fig. S55†).[41] *In situ* IR spectroscopy (poly(D-**Ox**-*alt*-**ITC1**) stirred in a THF solution of $Cu(OAc)_2{\cdot}H_2O$ at 50 °C) showed these vibrations increased at the same rate and plateaued after 135 minutes suggesting Cu^{2+} interacts through the thioimidate moiety of the imidothiocarbonate linkage (Fig. S57†).

Further evidence of bidentate coordination was observed by Raman spectroscopy analysis of polymer-Cu. An increase in intensity and broadening of the vibrational modes at 1620 cm^{-1} and 1380 cm^{-1}, corresponding to C=N and S–C vibrations respectively was observed, indicative of multiple coordination modes (Fig. 5A). Moreover, vibrational modes at 416 and 749 cm^{-1} were observed in both the Raman spectra of the polymer-Cu and $Cu(OAc)_2{\cdot}H_2O$, confirming Cu^{2+} adsorption to poly(D-**Ox**-*alt*-**ITC1**) and retention after washing.

Poly(D-**Ox**-*alt*-**ITC1**) was then stirred in the presence of different concentrations of $Cu(OAc)_2{\cdot}H_2O$ (0.33 and 0.066 mol L^{-1}) and the UV-vis spectrum of the original solution was compared to that of the supernatant. A decrease in absorbance at 740 nm was observed for each of the supernatants (28% at 0.33 mol L^{-1} and 67% at 0.066 mol L^{-1}) indicating a decrease in the concentration of the $Cu(OAc)_2{\cdot}H_2O$ in solution (Fig. 5B).

Thermogravimetric analysis was done to compare the percentage of residual char at 600 °C of the polymer-Cu and poly (D-**Ox**-*alt*-**ITC1**) (Fig. S56†). Decomposition of polymer-Cu resulted in a residual mass 5% greater than that of the poly(D-**Ox**-*alt*-**ITC1**), indicative of residual thermally stable Cu, likely copper oxides. As reported in literature, the thermal stability of poly(D-**Ox**-*alt*-**ITC1**) decreased upon coordination to Cu^{2+}, with comparison of the thermal degradation profile indicating multiple degradation pathways in polymer-Cu.[42] It is likely that Cu^{2+} catalyses the degradation of poly(D-**Ox**-*alt*-**ITC1**) at lower temperatures, however high thermal degradation temperatures are still maintained for polymer-Cu ($T_{d,5\%}$ = 234 and 278 °C for polymer-Cu and poly(D-**Ox**-*alt*-**ITC1** respectively).

Conclusions

The ROCOP of aromatic ITCs with an anhydro-functionalised xylofuranose derivative has been reported. Selectivity towards polymerisation and formation imidothiocarbonate linkages over formation of a cyclic thionocarbamate could be controlled through variation of the catalyst and reaction parameters. Kinetic studies showed a first order dependence of the reaction rate in oxetane monomer concentration, and a second order dependence on the concentration of binary catalyst/cocatalyst system (**AlTris** and PPNCl). All polyimidothiocarbonates showed high thermal stability ($T_{d,5\%}$ >228 °C) and high T_g (76–132 °C). Crosslinking with difunctional ITCs lead to increased T_gs. Chemical and photo degradation has also been demonstrated under acidic, basic and UV light conditions. Block copolymers could be synthesised through variation of the initiator as well as through exploitation of the living nature of ROCOP. Finally, initial studies showed the polymer could be used as a metal ion adsorbent for Cu^{2+}. Performances remain modest but call for further investigation into bio-derived and degradable polymers with high functional group content for metal coordination.

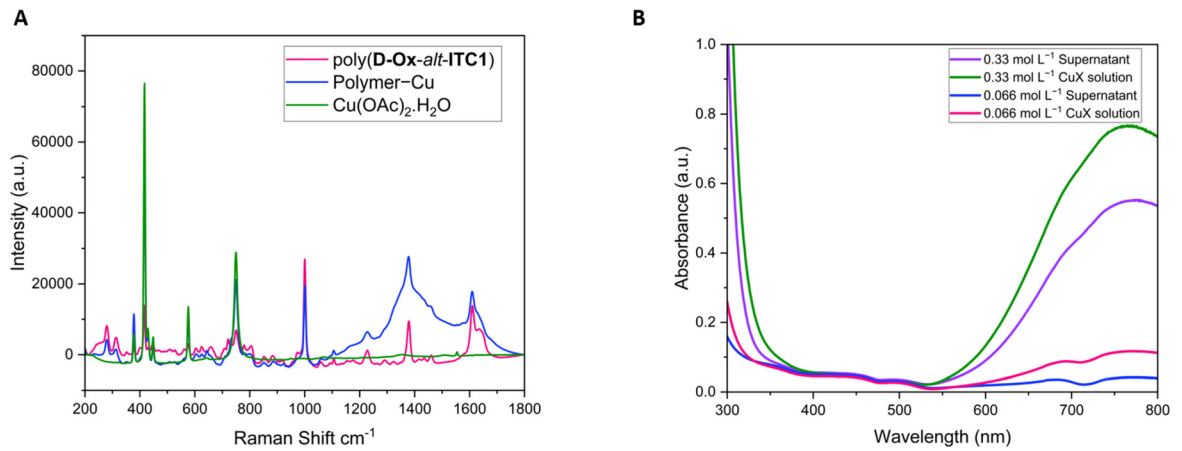

Fig. 5 Metal coordination to polymers. (A) Raman spectra of $Cu(OAc)_2{\cdot}H_2O$, polymer-Cu and poly(D-**Ox**-*alt*-**ITC1**). (B) UV-vis spectra of 0.33 and 0.066 mol L^{-1} aqueous $Cu(OAc)_2{\cdot}H_2O$ solutions before and after addition of polymer.

Conflicts of interest

There are no conflicts to declare.

Acknowledgements

The authors thank the Royal Society (UF/160021 and URF\R \221027: fellowship to A. B., RGF\R1\180036 studentship to E. F. C.) for research funding.

References

1 G. L. Gregory, E. M. López-Vidal and A. Buchard, *Chem. Commun.*, 2017, **53**, 2198–2217.
2 J. A. Galbis, M. D. G. García-Martín, M. V. De Paz and E. Galbis, *Chem. Rev.*, 2016, **116**, 1600–1636.
3 R. Xiao and M. W. Grinstaff, *Prog. Polym. Sci.*, 2017, **74**, 78–116.
4 J. J. Bozell and G. R. Petersen, *Green Chem.*, 2010, **12**, 539.
5 F. Fenouillot, A. Rousseau, G. Colomines, R. Saint-Loup and J. P. Pascault, *Prog. Polym. Sci.*, 2010, **35**, 578–622.
6 D. K. Schneiderman and M. A. Hillmyer, *Macromolecules*, 2017, **50**, 3733–3749.
7 J. Kawada, T. Lütke-Eversloh, A. Steinbüchel and R. H. Marchessault, *Biomacromolecules*, 2003, **4**, 1698–1702.
8 V. B. Purohit, M. Pięta, J. Pietrasik and C. M. Plummer, *Polym. Chem.*, 2022, **13**, 4858–4878.
9 E. Marianucci, C. Berti, F. Pilati, P. Manaresi, M. Guaita and O. Chiantore, *Polymer*, 1994, **35**, 1564–1566.
10 R. K. Sadhir and K. F. Schoch, *Chem. Mater.*, 1996, **8**, 1281–1286.
11 B. A. Fultz, D. Beery, B. M. Coia, K. Hanson and J. G. Kennemur, *Polym. Chem.*, 2020, **11**, 5962–5968.
12 C. Hardy, G. Kociok-Köhn and A. Buchard, *Chem. Commun.*, 2022, **58**, 5463–5466.
13 Z. Florjańczyk, D. Raducha and A. Kozera-Szałkowska, *Macromolecules*, 1996, **29**, 826–834.
14 C. Hardy, G. Kociok-Köhn and A. Buchard, *Polym. Chem.*, 2023, **14**, 623–632.
15 S. Rupf, P. Pröhm and A. J. Plajer, *Chem. Sci.*, 2022, **13**, 6355–6365.
16 A. J. Plajer and C. K. Williams, *Angew. Chem., Int. Ed.*, 2022, **61**, e202104495.
17 J. M. Longo, M. J. Sanford and G. W. Coates, *Chem. Rev.*, 2016, **116**, 15167–15197.
18 T. Lai, P. Zhang, J. Zhao and G. Zhang, *Macromolecules*, 2021, **54**, 11113–11125.
19 L. Song, M. Liu, D. You, W. Wei and H. Xiong, *Macromolecules*, 2021, **54**, 10529–10536.
20 C. Chen, Y. Gnanou and X. Feng, *Macromolecules*, 2021, **54**, 9474–9481.
21 D. Silbernagl, H. Sturm and A. J. Plajer, *Polym. Chem.*, 2022, **13**, 3981–3985.
22 X.-F. Zhu, R. Xie, G.-W. Yang, X.-Y. Lu and G.-P. Wu, *ACS Macro Lett.*, 2021, **10**, 135–140.
23 X. F. Zhu, G. W. Yang, R. Xie and G. P. Wu, *Angew. Chem., Int. Ed.*, 2022, **61**, e202115189.
24 A. J. Plajer, *ChemCatChem*, 2022, **14**, e202200867.
25 T. M. McGuire, J. Bowles, E. Deane, E. H. E. Farrar, M. N. Grayson and A. Buchard, *Angew. Chem., Int. Ed.*, 2021, **60**, 4524–4528.
26 T. Uryu, Y. Koyama and K. Matsuzaki, *Makromol. Chem.*, 1984, **185**, 2099–2107.
27 D. K. Tran, A. Z. Rashad, D. J. Darensbourg and K. L. Wooley, *Polym. Chem.*, 2021, **12**, 5271–5278.
28 T. M. McGuire and A. Buchard, *Polym. Chem.*, 2021, **12**, 4253–4261.
29 T. M. McGuire, E. F. Clark and A. Buchard, *Macromolecules*, 2021, **54**, 5094–5105.
30 M. Jurrat, B. J. Pointer-Gleadhill, L. T. Ball, A. Chapman and L. Adriaenssens, *J. Am. Chem. Soc.*, 2020, **142**, 8136–8141.
31 C. Hu, X. Chen, M. Niu, Q. Zhang, R. Duan and X. Pang, *Macromolecules*, 2022, **55**, 652–657.
32 M. J. Sanford, L. Peña Carrodeguas, N. J. Van Zee, A. W. Kleij and G. W. Coates, *Macromolecules*, 2016, **49**, 6394–6400.
33 L. Peña Carrodeguas, C. Martín and A. W. Kleij, *Macromolecules*, 2017, **50**, 5337–5345.
34 F. D. Monica and A. W. Kleij, *ACS Sustainable Chem. Eng.*, 2021, **9**, 2619–2625.
35 J. Burés, *Angew. Chem., Int. Ed.*, 2016, **55**, 2028–2031.
36 J. González-Fabra, F. Castro-Gómez, A. W. Kleij and C. Bo, *ChemSusChem*, 2017, **10**, 1233–1240.
37 F. Gorginpour, S. Moradinia, M. Daneshi and H. Zali-Boeini, *Ind. Eng. Chem. Res.*, 2022, **61**, 3694–3703.
38 S. Ravi, P. Puthiaraj, K. H. Row, D.-W. Park and W.-S. Ahn, *Ind. Eng. Chem. Res.*, 2017, **56**, 10174–10182.
39 S. Ravi and W.-S. Ahn, *Microporous Mesoporous Mater.*, 2018, **271**, 59–67.
40 L. Wang, J. Zhang, J. Sun, L. Zhu, H. Zhang, F. Liu, D. Zheng, X. Meng, X. Shi and F.-S. Xiao, *ChemCatChem*, 2013, **5**, 1606–1613.
41 S. Wang, S. Ma, Q. Li, X. Xu, B. Wang, K. Huang, Y. liu and J. Zhu, *Macromolecules*, 2020, **53**, 2919–2931.
42 R. Antony, S. Theodore David Manickam, K. Saravanan, K. Karuppasamy and S. Balakumar, *J. Mol. Struct.*, 2013, **1050**, 53–60.
43 H. Shirakura, Y. Hijikata, J. Pirillo, T. Yoneda, Y. Manabe, M. Murugavel, Y. Ide and Y. Inokuma, *Eur. J. Inorg. Chem.*, 2021, **2021**, 1705–1708.
44 B. De Bruin, E. Bill, E. Bothe, T. Weyhermüller and K. Wieghardt, *Inorg. Chem.*, 2000, **39**, 2936–2947.
45 G. Nasr, T. Macron, A. Gilles, Z. Mouline and M. Barboiu, *Chem. Commun.*, 2012, **48**, 6827–6829.
46 F. García, J. Pelss, H. Zuilhof and M. M. J. Smulders, *Chem. Commun.*, 2016, **52**, 9059–9062.
47 N. A. A. Qasem, R. H. Mohammed and D. U. Lawal, *npj Clean Water*, 2021, **4**, 36.